p-^{3}He Elastic Scattering from 13 to 20 MeV*

R. L. Hutson, Nelson Jarmie, J. L. Detch, Jr.,† and J. H. Jett
Los Alamos Scientific Laboratory, University of California, Los Alamos, New Mexico 87544
(Received 8 March 1971)

Accurate differential cross sections for protons elastically scattered by ^{3}He are presented for bombarding energies of 13.600, 16.232, and 19.480 MeV. The data have relative errors on the order of 0.7% and a scale error of 0.4%. The results are compared with the work of others and phase-shift analyses are briefly discussed.

I. INTRODUCTION

Experimental information on the mass-4 nuclear system has increased rapidly in the last few years.[1] Much of the detailed nuclear scattering information up to 20 MeV has been in the isospin $T_3 = 1$ mirror systems, $n+t$ and $p+{}^3$He, although the $T_3 = 0$ channels, $t+p$, $d+d$, $n+{}^3$He, have also received attention.[2] In the 10–20-MeV bombarding energy region for $p+{}^3$He elastic scattering, enough measurements have been made that a unique and understandable phase-shift analysis has become a possibility. Tivol[3] has measured proton polarizations in a range of energies from 11.6–21.3 MeV. Morales and Cahill[4] have measured cross sections at 18.0 and 19.8 MeV, and Vanetsian and Fedchenko[5] have reported cross-section data at 19.4 MeV. Recently, Morales and Cahill[4] have measured improved cross sections from 20.0–57.0 MeV. Baker *et al.*[6] at Saclay have measured ^{3}He polarizations as well as the spin correlations A_{xx} and A_{yy} at 19.4 MeV. Cahill *et al.*[7] determined proton polarizations at 19.4 MeV. Watt and Leland[8] have measured ^{3}He polarizations at 12.4, 14.9, and 16.2 MeV. There are also some early measurements at 14.5 MeV for the cross sections[9] and proton polarizations[10] by Rosen and Leland. The data below 12 MeV are summarized in Refs. 1 and 11. There appeared a need for accurate cross-section measurements between 12 and 19 MeV to help make headway in the phase-shift analysis, and this need motivated the present work. We have measured angular distributions of the elastic scattering of protons by ^{3}He at 13.600, 16.232, and 19.480 MeV to an average relative error of 0.7% and a scale error of 0.4%. The energies were chosen to match existing spin-dependent measurements. Some of the data have been previously reported.[12] Phase-shift analysis in this energy region has been attempted in Refs. 3, 6, and 8 and by ourselves[13] and Cahill.[14]

II. EXPERIMENTAL EQUIPMENT

A. Introduction

Figure 1 shows the configuration of the proton beam, target, Faraday cup, detectors, and scattering chamber. Instruments for monitoring ^{3}He temperature and pressure in the target, detector preamplifiers, and the target gas handling manifolds were in close proximity to the scattering chamber. The remaining electronics for processing the detector pulses, a SDS-930 computer for preliminary on-line data analysis, and the remaining control and monitoring equipment were located in a separate control room. Since detailed information on the equipment used and the tests performed to assure the desired accuracy was attained is available elsewhere,[2,15] only a brief description of the experimental apparatus will follow.

B. Beam and Beam Optics

The proton beam was accelerated through one or two of the Los Alamos Scientific Laboratory Van de Graaff accelerators. The proton energy was selected by using a 90°, double-focusing bending magnet together with momentum-selection slits. An array of slits, steering magnets, and quadrupoles was used to form a beam less than 1.0-mm wide and less than 1.5-mm high at the entrance to the target assembly. At the target entrance the beam was nearly parallel, having an emittance of less than 0.13 mrad cm in both the vertical and horizontal planes.

Upstream from the target were three alignment

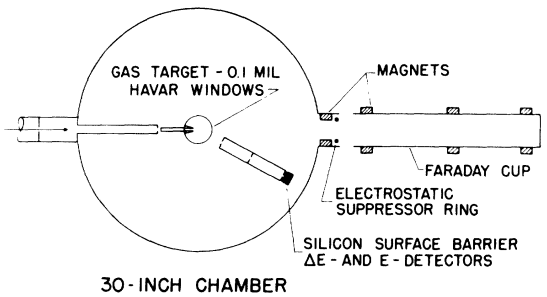

FIG. 1. Simplified drawing of the scattering chamber, final beam-defining apertures, target, Faraday cup, and detector telescope with collimators.

apertures at distances of 17.1, 51.4, and 127.6 cm, respectively, from the target center. By continuously monitoring the beam current on each of these apertures, it was possible to obtain nearly 100% transmission through the combination. Slight changes of the steering or quadrupole magnets from the optimum settings showed that the beam very nearly filled the apertures and that the beam axis was therefore within $\pm 0.06^\circ$ of the aperture-pair centerline. During a combination of measurements at the same scattering angle to both the left and right, the beam wandered less than $\pm 0.02^\circ$.

C. Faraday Cup and Charge Collection

In order to measure the total number of protons passing through the target during a scattering cross-section measurement, a tantalum-backed, water-cooled Faraday cup was placed behind the target. The Faraday cup was carefully designed so that the opening was wide enough to collect all the beam, the δ rays from the target were eliminated, and the secondary electrons from the beam stop were contained.

D. Scattering Chamber

A scattering chamber having a 30-in. i.d. was used. It was evacuated with a trapped oil-diffusion pump which usually maintained a chamber pressure of 5×10^{-7} Torr. The moving parts of the chamber will be discussed in the sections on the target and detectors.

E. Target and Gas Handling System

The gas target assembly was machined from solid brass into the form of a 9.3-cm-diam cylinder having a target volume of this diameter and height of about 1.6 cm. The containing foil was a 2.3-μm (0.09 mil) Havar. With the beam entering the target through a hole in the support post, the usable scattering angles were in the range of $\pm 168^\circ$. The gas system was evacuated and the target then filled with spectroscopic grade ^{3}He. The resulting target gas purity was 99.2%, or higher. The gas always contained 0.25% ^{4}He.

F. Temperature and Pressure Measurements

A Chromel-Alumel thermocouple, attached to the brass target assembly, was used to monitor the temperature of the gas during each scattering measurement. The temperature was continuously recorded on a Brown strip chart recorder. A diaphragm capacitance-bridge-type pressure transducer was used to monitor the target gas pressure. The voltage output from this transducer was measured with digital voltmeters. As a cross check, a mechanical diaphragm-type pressure gauge was included in the gas manifold system. The mechanical-gauge readings were within 0.3 Torr of the transducer readings.

G. Detector System

A particle telescope comprised of three silicon surface-barrier detectors of approximate thicknesses of 40, 250, and 2000 μm and areas of 100, 150, and 150 mm^2, respectively, provided energy measurement and mass identification of the scattered protons.

The full width at half maximum (FWHM) of the proton scattering angles accepted by the detectors was defined by a collimator comprised of a pair of nickel slits. The collimator-detector assembly was positioned in a precisely machined radial slot in the rotating turntable which served as the floor of the scattering chamber. The scattering angle was defined by the collimating system to within 0.4 and 0.7° FWHM at forward angles and backward angles, respectively. This width included contributions from foil multiple scattering, the 0.3° acceptance of the detector slits, and the incident proton beam divergence.

H. Electronics and Computer

Detector pulses were fed into charge-sensitive preamplifiers. The preamplifier signals then went into linear amplifiers which had dual outputs, one to provide energy information and the other to provide a signal for the coincidence circuits. The ΔE and E-ΔE signals were summed, digitized by analog-to-digital converters (ADC), and interfaced to an SDS-930 computer, which operated on-line during the experiment. Mass discrimination of the detected particles was done by accepting the sum pulse only if the quantity

$$N_M = a[(E+\Delta E)^n - E^n] \propto M^{n-1}Z^2,$$

was within predetermined mass gate limits.

The ADC's were gated open when signals from appropriate pairs of detectors in the telescope were in coincidence. Crossover timing was used

TABLE I. Errors.

Scale		Relative	
Source	% Error	Source	% Error
Pressure	0.1	Yield	$1/\sqrt{N}$
Temperature	0.07	Background	~0.1
Purity	0.1–0.2	Dead time	0.0–0.06
G	0.2		
N_b	0.2		

in the coincidence circuit which had a resolving time of 1 μsec. Accidental coincidences, which were measured by delaying one of the pulses, were never observed at the counting rates used.

III. DATA ANALYSIS AND ERRORS

The spectra for each run were analyzed for the number of counts in the peak by summing across the peak and subtracting a linear background. The ratio of peak to background was typically 100 to 1 and the error in the background was on the order of 0.1% of the peak total. Small dead-time and detector-efficiency corrections were made.

The target gas density was computed from the pressure and temperature measurements made for each run and corrected for the impurities in the gas. The impurity fraction was determined by measuring the yield of elastically scattered protons and comparing with known cross sections. The gas was typically 99.6% ^{3}He, 0.25% ^{4}He, and the balance air. The number of scattering centers per cubic centimeter was known to ±0.25%.

The solid angle or "G factor" for the detector system was determined by measuring the slit dimensions and using the formula of Silverstein.[16] The error was ±0.2% and only the lowest-order term of the Silverstein relation was used as the higher-order corrections were calculated to be negligible.

The beam current was measured in a Faraday cup described earlier. The integrator was calibrated with a precision current source and the resulting beam current was known to ±0.2% including the effects of multiple scattering, δ rays, and secondary electrons.

Cross sections were calculated for each run and then the corresponding left- and right-angle runs were averaged. This reduced the uncertainty in the knowledge of the zero angle, since the included angles were known to ±0.03°. For angles less than 35° lab, the ^{3}He and ^{4}He elastic scattering peaks were not kinematically separated enough to allow resolution of the two peaks. Thus for those angles an appropriate amount was subtracted from the apparent cross section. The error introduced by this was negligible.

A summary of the errors is contained in Table I. They have been separated according to whether they contribute to the relative or scale error. The absolute error may be found by combining the relative and scale errors according to

$$(\text{Rel. error})^2 + (\text{Scale error})^2 = (\text{Abs. error})^2 .$$

TABLE II. Differential cross sections p + ^{3}He elastic scattering, 13.600 MeV.

θ_{lab} (deg)	$\sigma(\theta)_{lab}$ (mb/sr)	$\theta_{c.m.}$ (deg)	$\sigma(\theta)_{c.m.}$ (mb/sr)	Relative error (%)	Absolute error (%)
12.00	351.7	16.03	199.0	0.77	0.85
15.00	336.4	20.01	191.7	0.58	0.69
20.00	339.4	26.63	196.3	0.53	0.65
25.00	321.2	33.20	189.4	0.51	0.63
30.00	289.7	39.72	174.9	0.50	0.62
35.00	252.0	46.16	156.4	0.53	0.65
40.00	213.6	52.52	136.8	0.55	0.66
45.00	172.7	58.80	114.7	0.52	0.64
50.00	137.9	64.97	95.26	0.50	0.62
55.00	105.4	71.03	76.05	0.51	0.63
60.00	78.73	76.97	59.55	0.51	0.63
65.00	57.41	82.78	45.66	0.55	0.66
70.00	40.70	88.45	34.14	0.72	0.81
75.00	27.32	93.98	24.25	0.74	0.83
80.00	18.47	99.36	17.38	0.74	0.82
85.00	12.38	104.59	12.37	0.75	0.83
90.00	8.667	109.66	9.212	1.21	1.27
100.00	7.679	119.34	9.255	1.28	1.33
110.00	11.57	128.42	15.80	0.98	1.05
120.00	17.27	136.92	26.58	0.78	0.86
130.00	23.57	144.92	40.48	0.70	0.79
140.00	28.83	152.47	54.47	0.59	0.69
150.00	33.11	159.67	67.62	0.51	0.63
160.00	36.14	166.60	78.18	0.53	0.65
165.00	36.78	169.99	81.20	0.51	0.63
168.00	37.29	172.00	83.12	1.01	1.08

TABLE III. Differential cross sections p + ^{3}He elastic scattering, 16.232 MeV.

θ_{lab} (deg)	$\sigma(\theta)_{lab}$ (mb/sr)	$\theta_{c.m.}$ (deg)	$\sigma(\theta)_{c.m.}$ (mb/sr)	Relative error (%)	Absolute error (%)
10.00	331.6	13.37	186.8	1.90	1.90
12.00	290.8	16.03	164.4	0.70	0.90
15.00	291.0	20.02	165.6	0.52	0.70
20.00	301.6	26.64	174.2	0.37	0.58
25.00	283.0	33.21	166.6	0.35	0.56
30.00	250.4	39.73	150.9	0.40	0.60
35.00	214.8	46.17	133.2	0.45	0.62
40.00	178.5	52.54	114.3	0.37	0.58
45.00	145.1	58.82	96.31	0.44	0.61
50.00	113.2	64.99	78.15	0.53	0.68
55.00	86.57	71.05	62.46	0.51	0.66
60.00	65.01	76.99	49.16	0.51	0.66
65.00	46.62	82.80	37.09	0.53	0.68
70.00	32.86	88.47	27.57	0.60	0.74
75.00	22.45	94.00	19.93	0.75	0.86
80.00	14.95	99.38	14.07	0.87	0.97
90.00	6.70	109.68	7.12	1.19	1.27
100.00	5.18	119.36	6.24	1.90	1.90
110.00	7.33	128.43	10.01	1.16	1.24
120.00	11.65	136.94	17.93	0.99	1.07
130.00	16.64	144.93	28.59	0.78	0.88
140.00	21.01	152.48	39.71	0.70	0.81
150.00	24.68	159.68	50.42	0.68	0.80
160.00	27.52	166.60	59.58	0.63	0.76
165.00	28.51	169.99	62.95	0.52	0.67
170.00	28.51	173.35	63.90	0.46	0.63

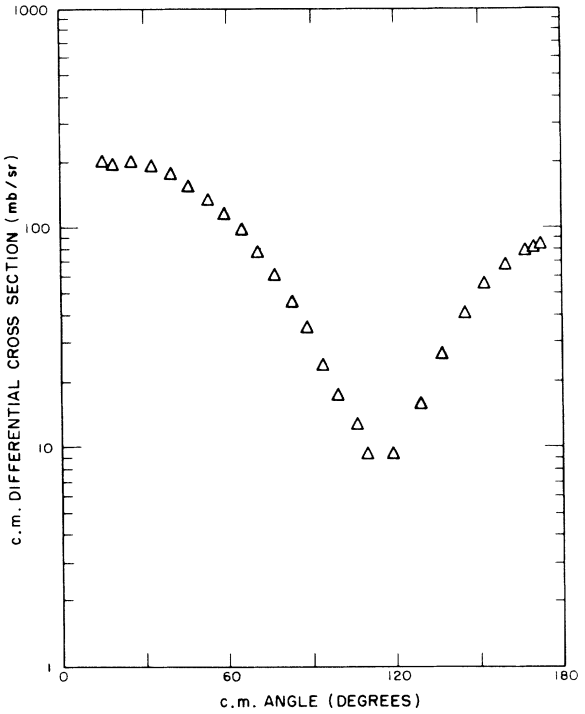

FIG. 2. p-^{3}He elastic scattering cross section at 13.600 MeV. The error bars are smaller than the points denoting the data.

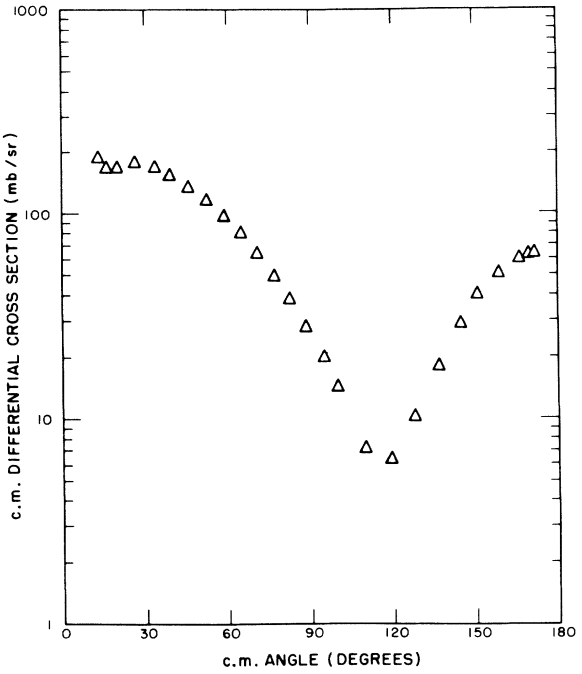

FIG. 3. p-^{3}He elastic scattering cross section at 16.232 MeV. The error bars are smaller than the points denoting the data.

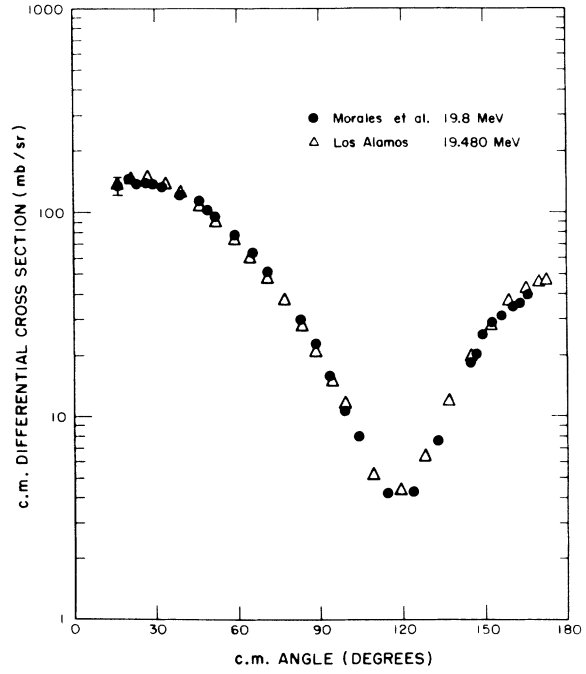

FIG. 4. Comparison of 19.48-MeV p-^{3}He elastic scattering data of Los Alamos with the 19.8-MeV data of Morales and Cahill (Ref. 4). Unless shown, the error bars are smaller than the plotting points.

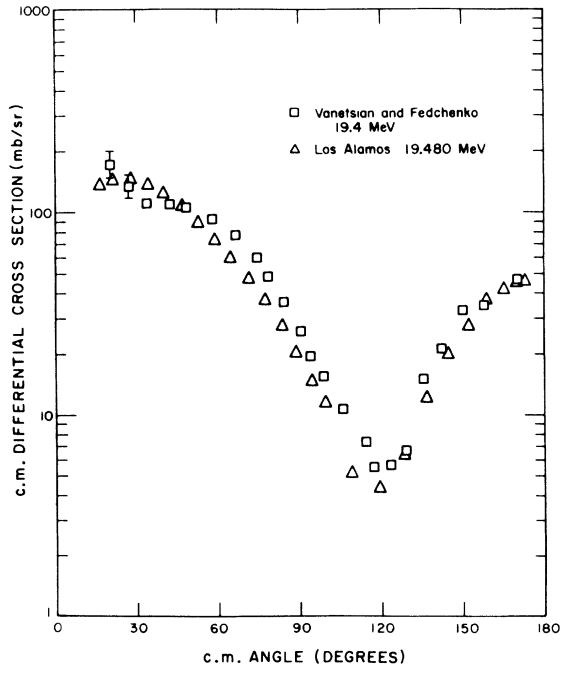

FIG. 5. Comparison of the 19.480-MeV p-^{3}He elastic scattering data of Los Alamos with the 19.4-MeV data of Vanetsian and Fedchenko (Ref. 5). Unless shown, the error bars are smaller than the plotting points.

TABLE IV. Differential cross sections p + ^{3}He elastic scattering, 19.480 MeV.

θ_{lab} (deg)	$\sigma(\theta)_{lab}$ (mb/sr)	$\theta_{c.m.}$ (deg)	$\sigma(\theta)_{c.m.}$ (mb/sr)	Relative error (%)	Absolute error (%)
12.00	241.7	16.04	136.4	0.55	0.66
15.00	251.9	20.04	143.2	0.55	0.67
20.00	255.4	26.66	147.4	0.51	0.64
25.00	233.2	33.24	137.2	0.48	0.61
30.00	204.9	39.76	123.5	0.54	0.65
35.00	172.2	46.21	106.7	0.51	0.64
40.00	139.2	52.58	89.05	0.52	0.64
45.00	110.5	58.85	73.31	0.54	0.80
50.00	86.64	65.03	59.68	0.55	0.81
55.00	65.43	71.09	47.18	0.57	0.82
60.00	48.04	77.03	36.32	0.56	0.82
65.00	34.73	82.85	27.62	0.68	0.90
70.00	24.21	88.52	20.31	0.83	1.02
75.00	16.67	94.05	14.79	0.83	1.02
80.00	10.78	99.43	10.15	1.18	1.24
90.00	4.790	109.73	5.095	1.32	1.37
100.00	3.193	119.40	3.853	1.81	1.85
110.00	4.632	128.47	6.336	1.36	1.41
120.00	7.722	136.97	11.91	1.13	1.19
130.00	11.14	144.96	19.17	0.93	1.00
140.00	14.78	152.50	27.99	0.85	0.93
150.00	17.71	159.69	36.24	0.71	0.80
160.00	20.14	166.61	43.65	0.59	0.67
165.00	20.83	170.00	46.10	0.62	0.72
168.00	21.00	172.01	46.93	0.62	0.72

IV. DATA

The data are tabulated in Tables II, III, and IV and are presented graphically in Figs. 2–5. In the tables are listed the lab angle (known to ±0.03°) for each datum, the lab cross section in mb/sr, the equivalent c.m. angle and cross section, along with the relative and absolute errors in standard deviations. The primary contribution to the relative errors is the statistics, with other sources of relative error contributing less than 0.2% in quadrature. The beam energy was known to ±15 keV with a spread of 20 keV FWHM.

V. DISCUSSION

Our data at 19.480 MeV are compared in Fig. 4 with that of Morales and Cahill.[4] There appears to be a slight systematic difference with angle, but the agreement looks good, especially in normalization. In Fig. 5, our data are compared with that of Vanetsian and Fedchenko.[5] They are in poor agreement in both shape and absolute normalization with differences as large as 50%. Considering the poor agreement not only here but in other reactions,[2] and that numerical data or detailed information is apparently unavailable, we feel that the data in Ref. 5 should no longer be used.

We have used our data with those of Refs. 8 and 3 to attempt a phase-shift analysis at 13.6 MeV. The results are similar (and similarly inconclusive) to the fits of others at other energies.[3,6,11,14] The S phases resemble hard-sphere phases; the P phases are broadly resonating; small amounts of D and F phases are necessary to fit the data. We obtain good fits, but a number of them are similar in type. Also, the errors in the phases are large. We shall not present any details here as we do not feel they are significant. Further data, or advances in phenomenological technique, such as an energy-dependent phase-shift analysis program,[17] are probably needed before a more unique phase-shift fit can be obtained.

ACKNOWLEDGMENTS

We have enjoyed various discussions and communications with T. A. Cahill and S. D. Baker. Our thanks to B. E. Watt and W. T. Leland for their data, and to D. C. Dodder for help with his analysis program. The experiment was greatly aided by the staff and operators of the accelerator facility. Lloyd Catlin, Robert Willis, and David Waymire assisted in parts of the experiment.

*Work performed under the auspices of the U. S. Atomic Energy Commission.

†Now at EG&G, Los Alamos, New Mexico 87544.

[1]W. E. Meyerhof and T. A. Tombrello, Nucl. Phys. A109, 1 (1968).

[2]J. L. Detch, Jr., Ph.D. thesis, University of Wyoming, 1970 (unpublished); Los Alamos Scientific Laboratory Report No. LA-4576, 1970 (unpublished); J. L. Detch, R. L. Hutson, N. Jarmie, and J. H. Jett, to be published.

[3]W. F. Tivol, University of California Lawrence Radiation Laboratory Report No. UCRL-18137, 1968 (unpublished).

[4]J. R. Morales and T. A. Cahill, Bull. Am. Phys. Soc. 14, 554 (1969); and private communication.

[5]R. A. Vanetsian and E. D. Fedchenko, At. Energ. (USSR) 2, 123 (1957) [transl.: Soviet J. At. Energy 2, 141 (1957)].

[6]S. D. Baker, T. A. Cahill, P. Catillon, J. Durand, and D. Garreta, Nucl. Phys. A160, 428 (1971).

[7]T. A. Cahill, P. Catillon, J. M. Durand, and D. Garreta, unpublished; the data are given in Ref. 6.

[8]B. E. Watt and W. T. Leland, private communication.

[9]L. Rosen and W. T. Leland, unpublished; and private communication.

[10]L. Rosen and W. T. Leland, Phys. Rev. Letters 8, 379 (1962).

[11]D. H. McSherry and S. D. Baker, Phys. Rev. C 1, 888 (1970).
[12]R. L. Hutson and N. Jarmie, Bull. Am. Phys. Soc. 14, 21 (1969); J. H. Jett, R. L. Hutson, J. L. Detch, Jr., and N. Jarmie, *ibid.* 15, 1661 (1970).
[13]N. Jarmie and J. H. Jett, Bull. Am. Phys. Soc. 15, 1661 (1970).
[14]T. A. Cahill, private communication.
[15]N. Jarmie, J. H. Jett, J. L. Detch, Jr., and R. L. Hutson, Phys. Rev. C 3, 10 (1971).
[16]E. A. Silverstein, Nucl. Instr. Methods 4, 53 (1959).
[17]D. Dodder, private communication.

PHYSICAL REVIEW C VOLUME 4, NUMBER 1 JULY 1971

Measurements of Six Light Masses

Lincoln G. Smith
Joseph Henry Laboratories, Princeton University, Princeton, New Jersey 08540
(Received 25 January 1971)

The mass differences of 16 doublets involving the six atoms H, D, ^{14}N, ^{16}O, ^{35}Cl, and ^{37}Cl have been measured with a new rf mass spectrometer with considerably greater precision than was attainable with the mass synchrometer. By least-squares adjustment, best values of the mass excesses of these six atoms have been determined for which the estimated errors are materially less than for previously published values.

APPARATUS AND PROCEDURE

Design considerations were presented in 1960[1] of the rf mass spectrometer,[2] then being proposed, which was used in the work reported here. A brief description of the instrument and its early performance was presented in 1967.[3]

A doublet spacing is measured by alternately displaying its two peaks on an oscilloscope screen at a rate of about (but not exactly) 15 peak pairs per second, i.e., by the familiar technique of visual peak matching. To make the orbit distributions of the two types of ion as nearly identical as possible, all voltages are alternated between pairs of values inversely proportional to the ionic masses. The two frequencies alternately applied to the modulator are generated by separate oscillators covering the range from 50 to 500 mHz, each being phase-locked to a multiple of 10 mHz derived from the same crystal-controlled oscillator plus or minus the frequency of a frequency synthesizer referenced to this same 10-mHz crystal. Each frequency may be set and read with respect to the other to less than 0.1 Hz, i.e., to a precision of a few parts in 10^{10}, which is quite adequate.

The two rf signals are fed to the modulator via tuned power amplifiers and tuned transmission lines. Each line contains a five-section low-pass filter to suppress overtones followed by a 3-dB pad and a tuning device known as a stub stretcher. The two tuners join, at a T, the single line leading to the modulator whose length is so adjusted that it is a quarter wavelength or very nearly so for one or both frequencies. This provides that a voltage node for one or both frequencies is at or very near the junction so that tuning adjustments to maximize both voltages at the modulator are very nearly independent. Of course, only one signal at a time is applied, the other being very completely suppressed by having the plate voltage removed from the last two of the three stages of the corresponding power amplifier by a fast-acting relay. These two relays, like those which control all dc voltages, are operated by a flip-flop circuit triggered by the sweep return signal from the display oscilloscope. Other switches similarly operated provide for differential gain control to set the peak heights accurately equal and for a 30 kHz square-wave signal to be applied to the second Y input of the oscilloscope on alternate sweeps. This signal splits the trace for one peak into two parallel traces between which the unsplit trace is centered by adjusting one synthesizer, as well as a number of other controls.

In order to display peaks, the frequency of the 10-mHz crystal oscillator may be swept by a small but adequate amount so that each frequency is swept by an amount proportional to that frequency. To avoid the small shift in either frequency that would otherwise result from phase slip in the phase detector of either phase-lock loop, an adjustable amount of sweep voltage is fed along with the phase detector output to the voltage-variable capacitor diode controlling each oscillator, of such magnitude that there is no sweep voltage discernable in said output and hence no phase slip in either phase detector. This means that each frequency would be swept the proper amount even if the gain of each loop were turned to zero. This